THE ROTATION OF IRREGULARLY SHAPED NATURAL SATELLITES IN THE SOLAR SYSTEM

Thomas Löeger and Maria G. Firneis
Institute of Astronomy
University of Vienna
Türkenschanzstrasse 17
A-1180 Vienna, Austria
T.Loeger@gmx.at

Abstract The temporal evolution of the rotational motion along with the attitude of a set of irregularly shaped small planetary satellites is studied. For this problem a computer application was developed featuring an FFT implementation scalable in terms of the available computer hardware optimized for fast execution, performed by reducing the amount of mass-storage operations with the aid of an adaptive multi-buffer cache strategy. Every satellite is modelled as a homogenous triaxial ellipsoid precessing under the torque of the main body. For a set of eight satellites the evolution of their spin-angular velocity vectors is numerically tracked using non-singular matrix differential equations. Calculations were carried out with a 4^{th} order Runge-Kutta algorithm using a grid of 1620 different initial conditions for the attitudes of the satellites. An FFT was applied to the results to observe, whether the spin axis tumbles chaotically in conjunction with chaotic rotation, or if the obliquity and the spin angular velocity remains constant or changes periodically for certain initial conditions. It is shown that for each satellite investigated a regular rotation is possible for spin axes with an obliquity near zero degrees. Other stable regions exist for each satellite as well. For Proteus, a satellite of Neptune, the stable region is maximally extended of all objects investigated.

Keywords: Satellites – Rotation – Stability

1. Introduction

The investigation of the temporal evolution of the spin-axes of natural satellites has a long history in celestial mechanics (see [11], [10], [14], [13], [6], [3], [7], [8]). The stability of the attitude of the rotation axes and the existence of resonant spin states is of special interest. All the above mentioned investigations have in common that a spin axis perpendicular to the orbital plane was

assumed. Thus only a small region in the phase space was investigated or the calculations were only carried out for one satellite.

Due to tidal forces rotational evolution tends to erect the spin axis until it is perpendicular to the orbital plane of the satellite. For some satellites these spin states however are not stable, e.g. for Hyperion. This behavior can only be found if a satellite is non-spherical, hence small in size. A numerical analysis of the stability of the attitude and the spin period of small, irregularly shaped natural satellites with an obliquity between 0 and 45 degrees with an unknown rotation state is presented in this work.

This analysis was performed with the aid of computer programs written in C# and Mathematica. This extensive program package can be used for further research tasks.

2. Theory

Many satellites' highly aspherical shapes can roughly by described as ellipsoidals. For the orientation of a satellite with respect to the main body two sets of coordinates are necessary; a reference frame and a body frame. The origins of both sets are situated in the satellites' center of mass. Every vector in the reference frame can be expressed in terms of the body frame with the aid of 3 right-hand rotations (through 3 Eulerian angles) around a sequence of (principal) body axes [4], [12]. Every rotation can be described by a 3x3 matrix with time-dependent elements. Consequently differential equations with the Eulerian angles as variables, describing the time development of the spin axis, are developed.

A body fixed coordinate system is given as follows. Let three vectors, $\overrightarrow{a}$, $\overrightarrow{b}$ and $\overrightarrow{c}$ define a right-hand set of axes fixed to the satellite which correspond to the principal moments of inertia $A \leq B \leq C$.

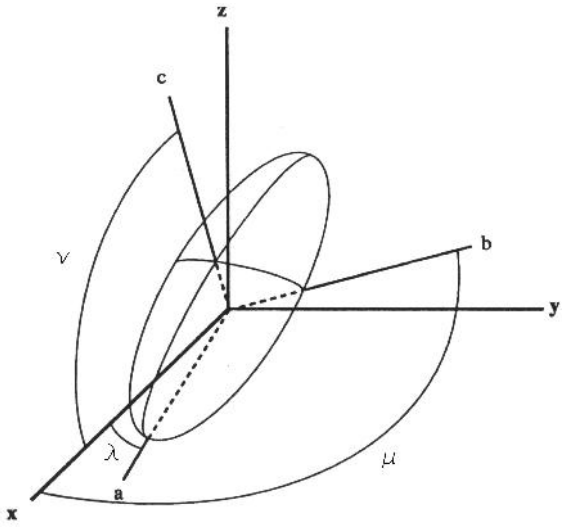

The reference coordinate system is given as follows. The trihedral $(\overrightarrow{x},\ \overrightarrow{y},\ \overrightarrow{z})$ is defined as:

$\overrightarrow{x}$ axis parallel to the planet-to-satellite vector,

$\overrightarrow{y}$ axis parallel to the orbital velocity,

$\overrightarrow{z}$ axis normal to the orbit of the satellite.

Starting with this reference system the trihedral system $\left(\overrightarrow{a},\ \overrightarrow{b},\ \overrightarrow{c}\right)$ is obtained through the rotation along the Eulerian angles $(\psi,\ \theta,\ \varphi)$:

At first the body axes are rotated around the $\overrightarrow{z}$ axis along an angle ψ, then around the new $\overrightarrow{x}$ axis (denoted by $\overrightarrow{x'}$) along an angle θ and finally around the new $\overrightarrow{z}$ axis (denoted by $\overrightarrow{c}$) along an angle φ.

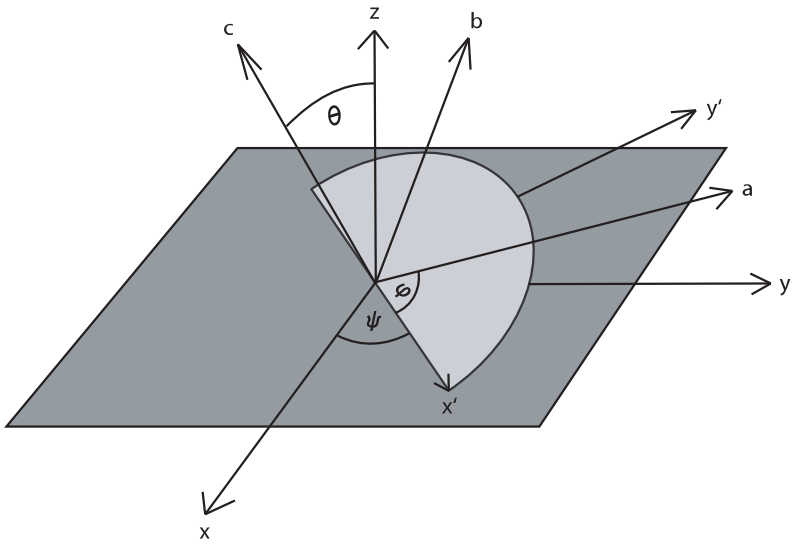

The axes $\overrightarrow{x},\ \overrightarrow{y}$ are rotated along the Eulerian angle ψ to give $\overrightarrow{x'},\ \overrightarrow{y'}$.

For the direction cosines $(\lambda,\ \mu,\ \nu)$ [6] one obtains:

$$\begin{aligned} \lambda &= \cos(\varphi)\cos(\psi) - \sin(\varphi)\cos(\theta)\sin(\psi), \\ \mu &= -\cos(\varphi)\sin(\psi) - \sin(\varphi)\cos(\theta)\cos(\psi), \\ \nu &= \sin(\theta)\sin(\varphi). \end{aligned} \tag{1}$$

With the components $(\omega_a,\ \omega_b,\ \omega_c)$ of the angular velocity vector referenced to the axes $\left(\overrightarrow{a},\ \overrightarrow{b},\ \overrightarrow{c}\right)$ the Eulerian equations can be written as [2]:

$$\begin{aligned} A\cdot\frac{\mathrm{d}\omega_a}{\mathrm{d}t} - (B-C)\cdot\omega_b\cdot\omega_c &= -\frac{3\cdot M\cdot G}{r^3}\cdot(B-C)\cdot\mu\cdot\nu, \\ B\cdot\frac{\mathrm{d}\omega_b}{\mathrm{d}t} - (C-A)\cdot\omega_c\cdot\omega_a &= -\frac{3\cdot M\cdot G}{r^3}\cdot(C-A)\cdot\nu\cdot\lambda, \\ C\cdot\frac{\mathrm{d}\omega_c}{\mathrm{d}t} - (A-B)\cdot\omega_a\cdot\omega_b &= -\frac{3\cdot M\cdot G}{r^3}\cdot(A-B)\cdot\lambda\cdot\mu. \end{aligned} \tag{2}$$

The equations in terms of the Eulerian angles experience a singularity however, when the spin axis is perpendicular to the orbital plane [5].

To circumvene this problem the attitude of the satellite with respect to its main body can be described as follows.

An initial coordinate system $(\overrightarrow{x},\ \overrightarrow{y},\ \overrightarrow{z})$ is given in such a way that the x axis is pointing from the main body to the perihelion of the satellites' orbit. The z axis is perpendicular to the $(x,\ y)$ plane originating in the center of the main body.

Let the principal moments of inertia be $(A,\ B,\ C)$. Three axis $\left(\overrightarrow{a},\ \overrightarrow{b},\ \overrightarrow{c}\right)$ parallel to these principal moments can be used to describe a coordinate system fixed to the satellite (body fixed coordinate system).

E_{ij} are the cosines of the angle between the i^{th} body fixed axis (a, b, or c) and the j^{th} initial axis (x, y, or z). The nine E_{ij}s represent a 3x3 rotation matrix E. With the aid of this matrix, every vector in the initial frame can be transformed to the corresponding vector in the body fixed (rotating) frame. Because of the orthogonality of E, the transposed matrix E^t describes the inverse transformation.

Let $\overrightarrow{l}$ be the torque and let $\overrightarrow{\omega}$ be the angular velocity vector of the satellite in the inertial frame.

Furthermore let $\overrightarrow{\sigma} \equiv \overrightarrow{\omega}\frac{\mathrm{d}t}{\mathrm{d}f}$ with f denoting the true anomaly. One can define $\overrightarrow{L} = E\overrightarrow{l}$ as torque and $\overrightarrow{\Omega} = E\overrightarrow{\omega}$ as the spin angular velocity vector in the body fixed frame, thus $\overrightarrow{\Sigma} \equiv \overrightarrow{\Omega}\frac{\mathrm{d}t}{\mathrm{d}f} = E\overrightarrow{\sigma}$.

The components of the torque in the body fixed coordinate system are:

$$L_A = A\,\Omega_A, \tag{3}$$

$$L_B = B\,\Omega_B, \tag{4}$$

$$L_C = C\,\Omega_C. \tag{5}$$

This leads to the following form of the Eulerian equations [5]:

$$\begin{aligned}
\frac{\mathrm{d}}{\mathrm{d}f}\Sigma_A &= \frac{\Sigma_A 2e\sin(f)}{1+e\cos(f)} - \alpha\Sigma_B\Sigma_C + \\
&\quad \frac{3\alpha\left(E_{21}\cos(f)+E_{22}\sin(f)\right)\left(E_{31}\cos(f)+E_{32}\sin(f)\right)}{1+e\cos(f)}, \\
\frac{\mathrm{d}}{\mathrm{d}f}\Sigma_B &= \frac{\Sigma_B 2e\sin(f)}{1+e\cos(f)} + \beta\Sigma_A\Sigma_C - \\
&\quad \frac{3\beta\left(E_{11}\cos(f)+E_{12}\sin(f)\right)\left(E_{31}\cos(f)+E_{32}\sin(f)\right)}{1+e\cos(f)}, \\
\frac{\mathrm{d}}{\mathrm{d}f}\Sigma_C &= \frac{\Sigma_C 2e\sin(f)}{1+e\cos(f)} - \gamma\Sigma_A\Sigma_B + \\
&\quad \frac{3\gamma\left(E_{11}\cos(f)+E_{12}\sin(f)\right)\left(E_{21}\cos(f)+E_{22}\sin(f)\right)}{1+e\cos(f)}.
\end{aligned} \tag{6}$$

With the following equations, one can describe the temporal evolution of the spin axis of a satellite with the aid of direction cosines:

$$\begin{aligned}
\frac{\mathrm{d}}{\mathrm{d}f}E_{11} &= \Sigma_C E_{21} - \Sigma_B E_{31}, \\
\frac{\mathrm{d}}{\mathrm{d}f}E_{21} &= \Sigma_A E_{31} - \Sigma_C E_{11}, \\
\frac{\mathrm{d}}{\mathrm{d}f}E_{31} &= \Sigma_B E_{11} - \Sigma_A E_{21}, \\
\frac{\mathrm{d}}{\mathrm{d}f}E_{12} &= \Sigma_C E_{22} - \Sigma_B E_{32}, \\
\frac{\mathrm{d}}{\mathrm{d}f}E_{22} &= \Sigma_A E_{32} - \Sigma_C E_{12}, \\
\frac{\mathrm{d}}{\mathrm{d}f}E_{32} &= \Sigma_B E_{12} - \Sigma_A E_{22}, \\
\frac{\mathrm{d}}{\mathrm{d}f}E_{13} &= \Sigma_C E_{23} - \Sigma_B E_{33}, \\
\frac{\mathrm{d}}{\mathrm{d}f}E_{23} &= \Sigma_A E_{33} - \Sigma_C E_{13}, \\
\frac{\mathrm{d}}{\mathrm{d}f}E_{33} &= \Sigma_B E_{13} - \Sigma_A E_{23}.
\end{aligned} \tag{7}$$

3. Numerical investigation

A computer program in C# was developed to numerically integrate the equations of motion. For this purpose a 4^{th} order Runge-Kutta [9] with variable

step-size was used. The results were analyzed by calculating a frequency spectrum using an optimized Fast Fourier (FFT) algorithm implemented by one of the authors of this treatise (T. Loeger). This implementation contains an intelligent multi-buffer cache strategy to reduce Hard-Disk operations.

To visualize the results, the program was designed to create Mathematica notebooks with dynamically structured plot-expressions. A specially designed notebook is used to read all these notebooks and execute them. After the paths to the output-files of the C# program are properly set, this notebook reads all the files and creates the plots showing the results of the integration. The formulae used by the application were set up by Mathematica.

It is sufficient to describe the initial attitude of a satellite in terms of two angles as initial conditions rather than using the elements of the rotation matrix E.

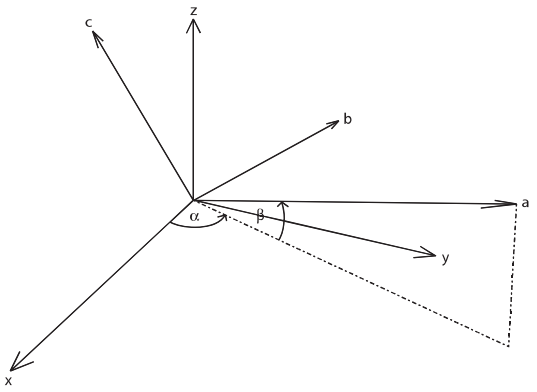

The angle α is varied between 0 and 180 degrees in steps of 5 degrees, β is varied between 0 and 45 degrees in steps of 1 degrees. The mean rotation period expressed in terms of the true anomaly (corresponding to normalization) was selected as the z-element of the spin angular velocity vector.

The variation of the spin axis attitude and the evolution of the spin angular velocity vector were calculated for 1620 initial conditions with a 4^{th} order Rung-Kutta algorithm.

An FFT was applied to the results obtained above. For each satellite and initial condition, a histogram over all the frequencies obtained in the Fourier-spectra was calculated. Histograms were used to distinguish the frequencies indicating resonant spin states and "noise"-frequencies.

For each satellite a plot for all initial conditions was created showing the values of the remaining frequency-peaks found for each initial condition (see Fig. 1 – Fig. 8).

4. Results

The frequency-values in terms of the orbital period were gray-coded as shown in Fig. 1 – Fig. 8. Left to each figure values markers of the correspond-

ing frequencies are displayed. Due to the fact, that the frequency corresponding to a certain gray-code differs for each satellite, these code plots cannot be directly compared, with the exception that black regions always indicate initial conditions for which the satellite's rotation state becomes chaotic. Each point in the plot corresponds to the result of one initial condition for α and β, where alpha is the azimuthal and beta the polar angle describing the initial attitude of the satellite (the initial conditions for the subsequent integration).

4.1 Satellites of Jupiter

4.1.1 Adrastea.

Physical and orbital characteristics	
Period of revolution [days]	0.29826
Eccentricity	0.0018
Mass of main body (Jupiter) [kg]	$1.899 \cdot 10^{27}$
Mass of satellite [kg]	$1.91 \cdot 10^{16}$
Diameter [km]	$25 \times 20 \times 15$

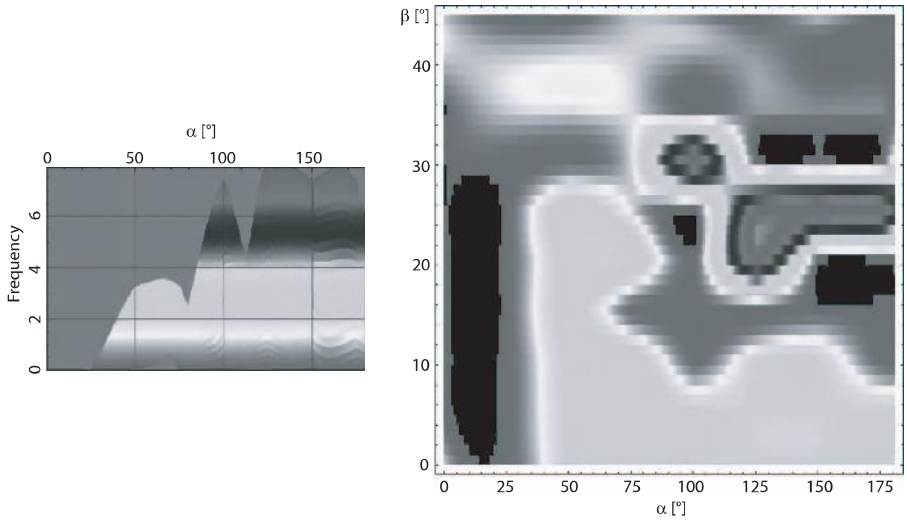

Figure 1. A plot showing the gray-coded values of the frequency-peaks found for all initial conditions (α,β) for Adrastea.

As one can see in Fig. 1 the eccentricity e is relatively large, leading to a large chaotic region for values of the azimuthal angle α between 10 and 20 degrees and the polar angle β between 0 and 30 degrees (black regions in the right plot of Fig. 1). Small regions of initial conditions leading to chaotic rotation can be found for alpha between 150 and 180 degrees and beta between 18 and 20 degrees and beta between 35 and 40 degrees. In the region of initial conditions leading to regular rotation states, one observes resonances between 2:1 and 3:1 for alpha between 50 and 180 degrees and beta between 0 and 20 degrees and

an approximate 1:1 resonance for alpha between 0 and 180 degrees and beta between 32 and 45 degrees.

4.2 Satellites of Saturn

4.2.1 Atlas.

Physical and orbital characteristics	
Period of revolution [days]	0.6019
Eccentricity	0
Mass of main body (Saturn) [kg]	$5.6846 \cdot 10^{26}$
Mass of satellite [kg]	$1.91 \cdot 10^{16}$
Diameter [km]	$18.5 \times 17.2 \times 13.5$

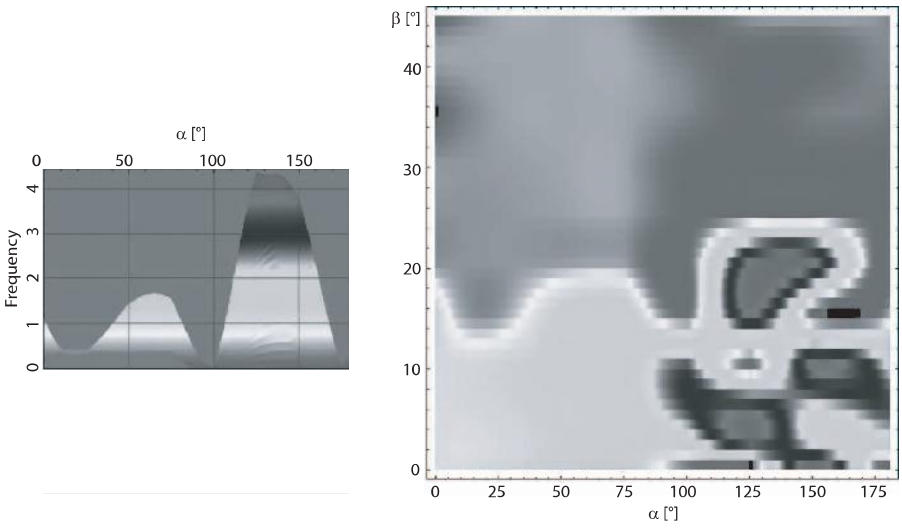

Figure 2. A plot showing the gray-coded values of the frequency-peaks found for all initial conditions (α,β) for Atlas.

The eccentricity e is zero, leading only to non-chaotic regions as one can observe in Fig. 2. One can find initial conditions leading to resonances between 1:1 and 2:1 for values of alpha between 0 and 80 degrees and beta between 0 and 15 degrees and 1:2 resonances for alpha between 0 and 80 degrees and beta between 20 and 45 degrees.

4.2.2 Prometheus.

Physical and orbital characteristics	
Period of revolution [days]	0.61299
Eccentricity	0.0024
Mass of main body (Saturn) [kg]	$5.6846 \cdot 10^{26}$
Mass of satellite [kg]	$3.3 \cdot 10^{17}$
Diameter [km]	$145 \times 85 \times 65$

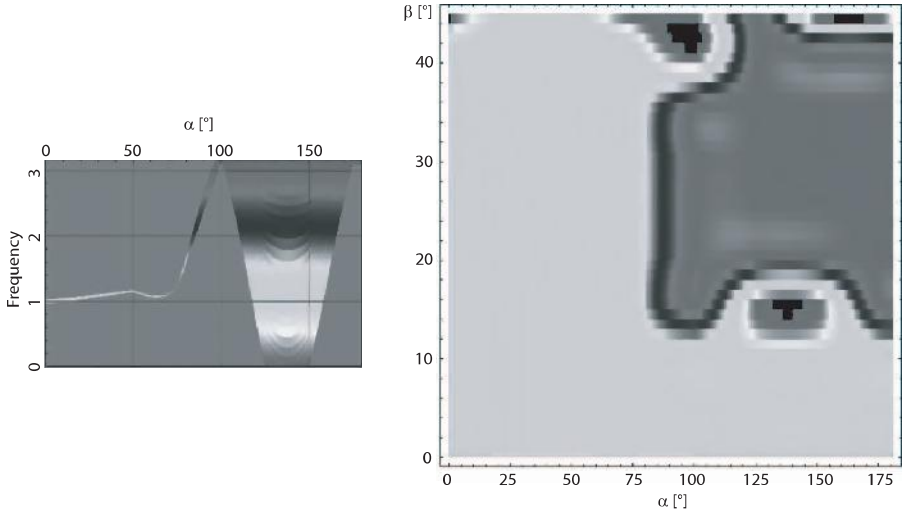

Figure 3. A plot showing the gray-coded values of the frequency-peaks found for all initial conditions (α,β) for Prometheus.

The eccentricity e is relatively small, leading to small chaotic regions for values of alpha between 110 and 120 degrees and for values of beta around 10 degrees, around values of alpha 70 degrees and 150 degrees, and values of beta between 35 and 45 degrees (shown black in Fig. 3). One can find large regions of initial conditions leading to 1:1 and 1:3 resonances for initial conditions for alpha between 0 and 180 degrees and for beta between 0 and 20 degrees, and further for alpha between 0 and 50 degrees and beta between 0 and 45 degrees.

4.2.3 Pandora.

Physical and orbital characteristics	
Period of revolution [days]	0.628
Eccentricity	0.0042
Mass of main body (Saturn) [kg]	$5.6846 \cdot 10^{26}$
Mass of satellite [kg]	$1.94 \cdot 10^{17}$
Diameter [km]	$114 \times 84 \times 62$

The eccentricity e is relatively large, leading to a large chaotic region for initial conditions for alpha between 0 and 10 degrees and beta between 20 and 30 degrees, and a small region for initial conditions for alpha of 100 and 130 degrees and values of beta for 25 and 40 degrees (black regions in Fig. 4). One can find initial conditions leading to resonances between 1:1 and 2:1 for initial conditions of alpha between 50 and 180 degrees and beta between 0 and 15 degrees.

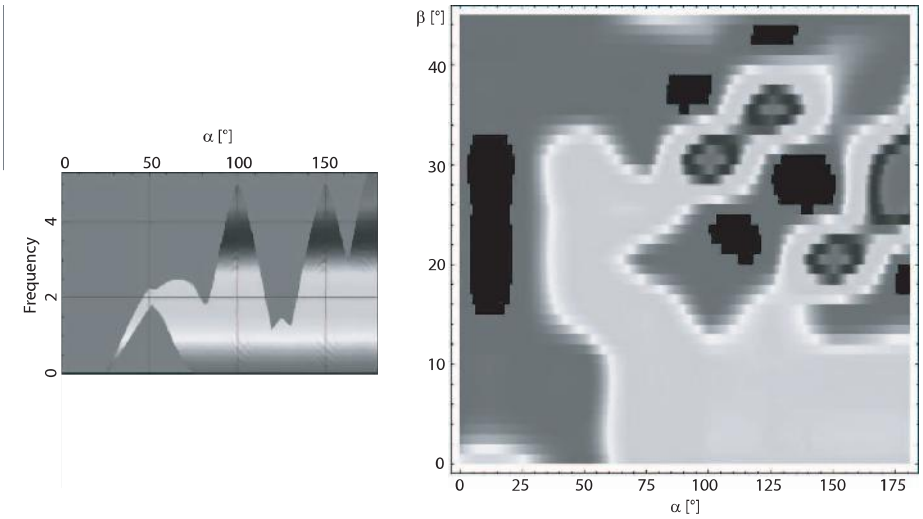

Figure 4. A plot showing the gray-coded values of the frequency-peaks found for all initial conditions (α,β) for Pandora.

4.2.4 Telesto.

Physical and orbital characteristics	
Period of revolution [days]	1.8878
Eccentricity	0
Mass of main body (Saturn) [kg]	$5.6846 \cdot 10^{26}$
Diameter [km]	$34 \times 28 \times 26$

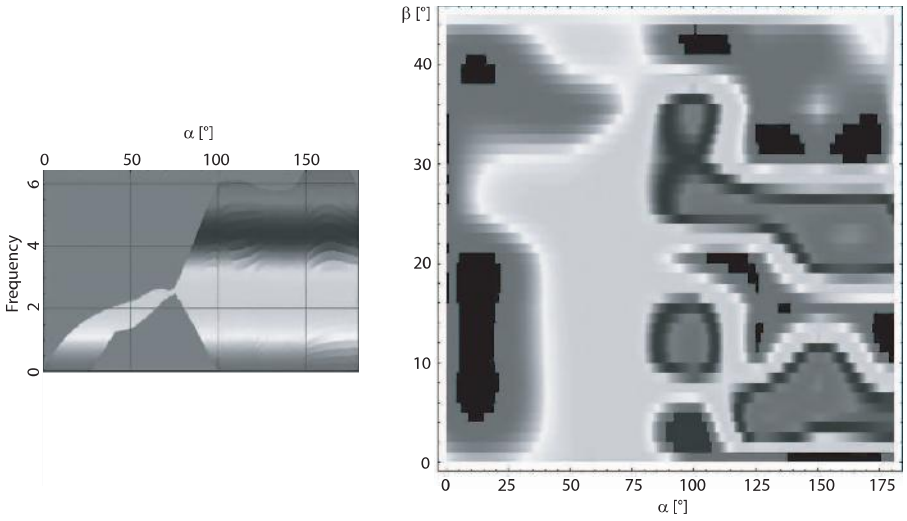

Figure 5. A plot showing the gray-coded values of the frequency-peaks found for all initial conditions (α,β) for Telesto.

Even if Telesto's eccentricity is zero, one can recognize many initial conditions leading to chaotic rotation, because Telesto is highly aspherical. These

regions can be found for alpha around 10, 100 and 180 degrees and for initial conditions for beta between 10 and 30 degrees, at 0 degrees and at 30 degrees (black regions in Fig. 5). A distinct region leading to a 1:2 resonance can be observed in the diagrams of Fig. 5 for values of alpha between 30 and 40 degrees and beta between 0 and 40 degrees.

4.2.5 Calypso.

Physical and orbital characteristics	
Period of revolution [days]	1.8878
Eccentricity	0
Mass of main body (Saturn) [kg]	$5.6846 \cdot 10^{26}$
Diameter [km]	$34 \times 22 \times 22$

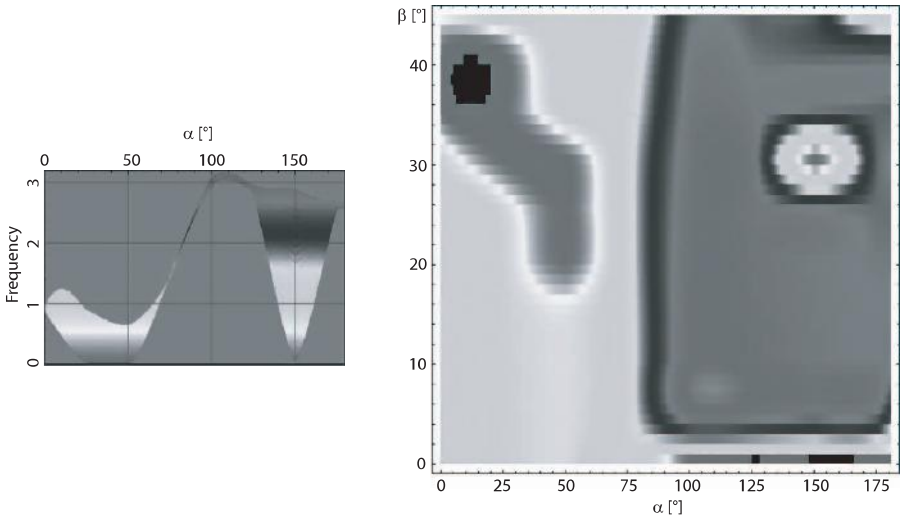

Figure 6. A plot showing the gray-coded values of the frequency-peaks found for all initial conditions (α,β) for Calypso.

Considering the very small eccentricity of Calypso, only a small chaotic region can be observed. This region can be found for initial conditions of alpha around 10 degrees and for beta around 35 degrees (black regions in Fig. 6). There is a large region of initial conditions leading to a 3:1 resonance for alpha between 70 and 180 degrees and beta between 5 and 45 degrees and a region of initial conditions leading to 1:1 resonances for alpha between 0 and 70 degrees and beta between 0 and 40 degrees.

4.2.6 Helene.

Physical and orbital characteristics	
Period of revolution [days]	2.7369
Eccentricity	0.0022
Mass of main body (Saturn) [kg]	$5.6846 \cdot 10^{26}$
Diameter [km]	$34 \times 22 \times 22$

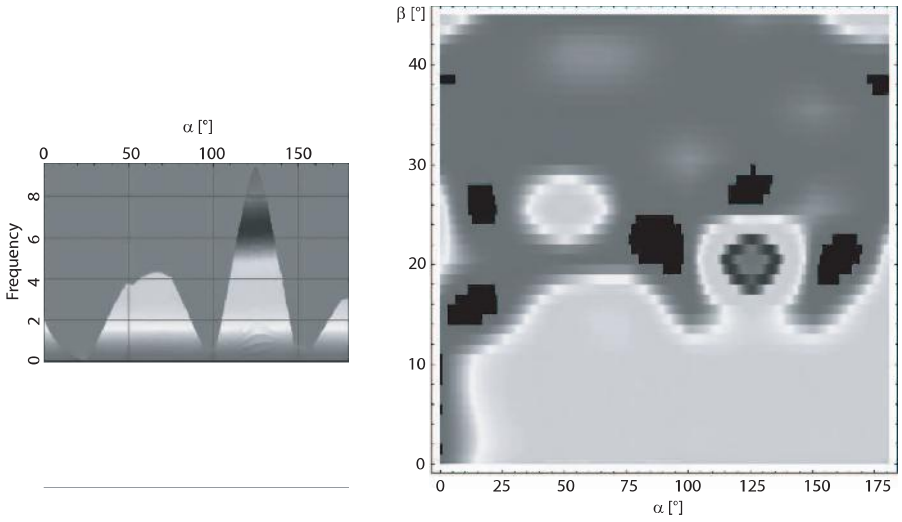

Figure 7. A plot showing the gray-coded values of the frequency-peaks found for all initial conditions (α,β) for Helene.

Even though the eccentricity of this satellite is small, some chaotic regions are visible, more precisely at alpha around 10 degrees, 80 degrees, 170 degrees and 180 degrees and beta around 20, 30 and 40 degrees (black regions in Fig. 7). There is a large region of initial conditions leading to resonances between 1:2 and 1:4 at alpha between 20 and 180 degrees and beta between 0 and 20 degrees, and a region leading to a 1:1 resonance for alpha between 0 and 180 degrees and beta greater than 25 degrees.

4.3 Satellites of Neptune

4.3.1 Proteus.

Physical and orbital characteristics	
Period of revolution [days]	1.122
Eccentricity	0.0022
Mass of main body (Neptune) [kg]	$1.0243 \cdot 10^{26}$
Mass of satellite [kg]	$5 \cdot 10^{19}$
Diameter [km]	$440 \times 416 \times 404$

Proteus is nearly spherical, but its orbit shows a small eccentricity, so there are some regions leading to chaotic rotation for initial conditions for alpha of 10 and 140 degrees and for beta at 15 and 40 degrees (black regions in the right plot above). A large region leading to a synchronous rotation state (1:1 resonance) can be observed for alpha between 0 and 180 degrees and beta between 0 and 15, respectively 45 degrees, as well as a region leading to a 3:1 resonance for alpha between 100 and 180 degrees and beta between 10 and 40 degrees.

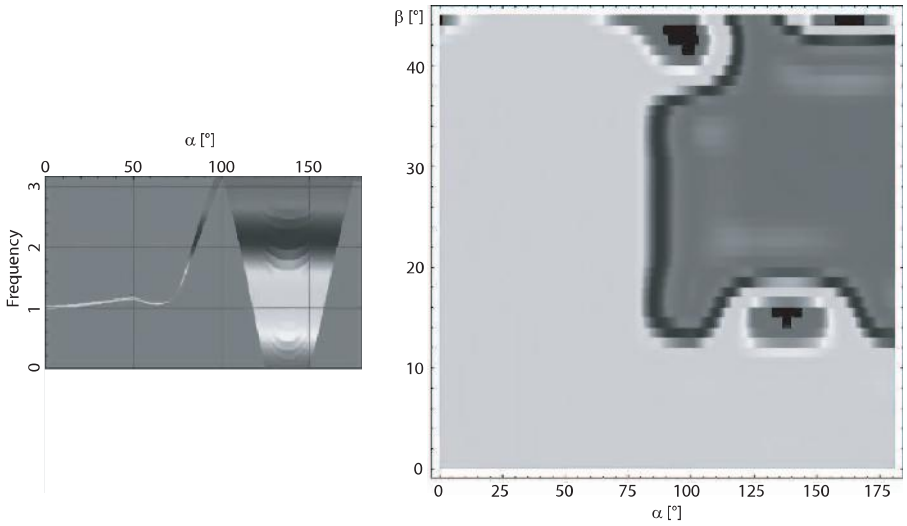

Figure 8. A plot showing the gray coded values of the frequency-peaks found for all initial conditions (α,β) for Proteus.

References

[1] Boehme, G. 1991, Algebra 7. Auflage,
Springer-Verlag, Berlin, Heidelberg, New York

[2] Danby, J. M. A. 1992, Fundamentals of Celestial Mechanics, Second Edition (Willmann-Bell)

[3] Dobrovolskis, R., Anthony 1995, Chaotic Rotation of Nereid?,
Icarus, **118**, 181-198

[4] Goldstein, H. 1950, Classical Mechanics,
Addison-Wesley, Reading, Mass.

[5] Julian, W. H. 1990, The Comet Halley nucleus: Random jets,
Icarus, **88**, 355-371

[6] Klavetter, James, Jay 1989, Rotation of Hyperion II Dynamics,
The Astronomical Journal, **98**, 5, 1855-1874

[7] Kouprianov, V. V., Shevchenko, I. I. 2002, On the chaotic rotation of planetary satellites: The Lyapunov spectra and the maximum Lyapunov exponents,
Astron. and Astrophysics, **394**, 663-674

[8] Kouprianov, V. V., Shevchenko, I. I. 2003, On the chaotic rotation of planetary satellites: The Lyapunov exponents and the energy,
Astron. and Astrophysics, **410**, 749-757

[9] Pang, Tao 1997, An Introduction to Computational Physics,
Cambridge University Press

[10] Peale, S. J., Rotation Histories of the natural Satellites
in Planetary Satellites, ed. Burns, J., A. 1977, 87-112

[11] Peale, S. J.: 1973, Rotation of Solid Bodies in the Solar System,
Reviews of Geophysics and Space Physics, **Vol 11**, No 4, 767-793

[12] Plummer, H. C. 1960, An Introductory Treatise on Dynamical Astronomy, Dover, NY

[13] Wisdom, J. 1987, Chaotic Dynamics in the Solar System, Icarus, **72**, 241-275

[14] Wisdom, J., Peale, S. J., Mignard, F. 1984, The chaotic rotation of Hyperion, Icarus, **58**, 137-152